文章编号: 1001 - 9014(2015)06 - 0688 - 06

DOI:10.11972/j.issn.1001 - 9014.2015.06.010

Zero-field spin splitting and high-field g-factor of an asymmetrical $In_{0.53}Ga_{0.47}As/In_{0.52}Al_{0.48}As$ quantum well

XU Yong-Gang[1], LV Meng[1], CHEN Jian-Xin[2], LIN Tie[1], YU Guo-Lin[1*], DAI Ning[1], CHU Jun-Hao[1]

(1. National Laborotary for Infrared Physics, Shanghai Institute of Tehcnical Physics, Chinese Academy of Sciences, Shanghai 200083, China;
2. Key Laboratory of Infrared Imaging Materials and Detectors, Shanghai Institute of Technical Physics, Chinese Academy of Sciences, Shanghai 200083, China)

Abstract: This paper investigated the magnetotransport properties of the two-dimensional electron system in an asymmetrical $In_{0.53}Ga_{0.47}As/In_{0.52}Al_{0.48}As$ quantum well, in which the expected beatings in the Shubinikov-de Haas oscillations of the longitudinal magnetoresistance R_{xx} were not observed. Zero-field spin splitting was extracted by measuring the weak anti-localization effect and the high field effective g-factor, g^*, was extracted by fitting the tilt angle θ-dependent spacing of spin-splitted R_{xx} peaks. The Dingle plot is shown to be nonlinear, which can be attributed to the long-range scattering potential from the doping Be atoms near the substrate.

Key words: two-dimensional electron system, InGaAs/InAlAs quatum well, zero-field spin splitting, g-factor
PACS: 71.18. +y, 71.70.Ej, 72.25.Dc, 73.21.Fg

非对称 $In_{0.53}Ga_{0.47}As/In_{0.52}Al_{0.48}As$ 量子阱的零场自旋分裂能与高场 g 因子

徐勇刚[1], 吕 蒙[1], 陈建新[2], 林 铁[1], 俞国林[1*], 戴 宁[1], 褚君浩[1]

(1. 中国科学院上海技术物理研究所 红外物理国家重点实验室, 上海 200083;
2. 中国科学院上海技术物理研究所 红外成像材料与器件重点实验室, 上海 200083)

摘要: 研究了非对称 $In_{0.53}Ga_{0.47}As/In_{0.52}Al_{0.48}As$ 量子阱中二维电子气的磁输运性质,所测量的样品的径向磁阻 R_{xx} 的 Shubinikov-de Haas 振荡没有呈现出拍频的特征。通过测量样品的反弱局域效应提取了其零场自旋分裂能并通过对自旋分裂的 R_{xx} 双峰间距随倾斜角度 θ 的依赖关系的拟合提取了高场下的有效 g 因子。样品的 Dingle plot 图呈现非线性的特征,这可以归因于来自样品衬底附近的掺杂 Be 原子的长程势散射效应。

关 键 词: 二维电子气; InGaAs/InAlAs 量子阱; 零场自旋分裂能; g 因子

中图分类号: O472 + .6 **文献标识码**: A

Introduction

Spin splitting plays an important role in determining the electronic properties of semicondutor materials and in enabling the implementation of spintronics[1]. It is well known that the Landau quantization of a two-dimensional electron system (2DES) gives rise to magnetic oscillations in physical quantities such as resistivity[2], capacitance[3], and tunnelling conductivity[4] due to oscillations in the density of states. The involvement of spin splitting will further modulate such oscillations. For example, in the presence of finite zero-field spin splitting, the Shubinikov-de Haas (SdH) oscillations of magnetore-

Received date: 2014 - 11 - 01, **revised date**: 2015 - 09 - 25 **收稿日期**:2014 - 11 - 01, **修回日期**:2015 - 09 - 25
Foundation items: Supported by Special Funds for Major State Basic Research under Project (2012CB619203, 2013CB922301), National Natural Science Foundation of China (11174306, 61290304), Innovation Program of Shanghai Institute of Technical Physics of the Chinese Academy of Sciences (Q-ZY-76)
Biography: XU Yong-Gang (1988-), male, Xiaogan China, Ph. D. Research field focus on the electron transport properties of semiconductors. E-mail: xyg88@mail.ustc.edu.cn
* **Corresponding author**: E-mail: yug@mail.sitp.ac.cn

sistivity will show a beating pattern due to the difference in carrier concentrations between the spin-up and spin-down subbands[5]. In high magnetic field where Zeeman splitting is large enough to eliminate the overlapping of spin-up and spin-down levels due to broadening of Landau levels (LLs), the single peak of oscillating magnetoresistivity will split to double peaks.

Among various materials and structures, InGaAs/InAlAs heterostructures or quantum wells (QWs) are of great importance, not only because they are the first prototypical platform for realizing spin field effect transistor (spin-FET)[6], but also for that they own a large Rashba spin-orbit interaction (SOI)[7] strength, which can be effectively tuned by applying external electric field via gate voltages[8]. The large Rashba SOI gives rise to zero-field spin splitting of the two-dimensional electron system (2DES) and thus leads to previously mentioned SdH beating effect as well as the weak anti-localization effect (WAL)[9]. However, these two effects do not always appear together as experimentally demonstrated here.

In this work, we investigated the magneto-transport properties of an asymmetrical InGaAs/InAlAs QW, in which the anticipated SdH beating effect due to zero-field spin splitting was absent. This sheds doubts on the prevailing explanation of this kind of origins of SdH beating effect[10]. The possible reasons are discussed below. We also looked into the effective g-factor in high magnetic field and obtained a strongly enhanced value by exchange interaction.

1 Experiment details

Our sample is an $In_{0.53}Ga_{0.47}As/In_{0.52}Al_{0.48}As$ quantum well grown by molecular beam epitaxy (MBE) on a semi-insulating InP(001) substrate. At first, a very thin buffer layer of Be-doped $In_{0.52}Al_{0.48}As$ was grown directly on the InP substrate. The doping density of Be was 5×10^{12} cm^{-2}, which was designed to pin the Fermi level of the structure slightly above the valence band maximum of undoped $In_{0.52}Al_{0.48}As$. Next, a sequence of $In_{0.52}Al_{0.48}As$ bottom barrier (350 nm), $In_{0.53}Ga_{0.47}As$ well (15 nm), Si δ-doped $In_{0.52}Al_{0.48}As$ upper barrier (30 nm) and a cap layer of $In_{0.53}Ga_{0.47}As$ (15 nm) were grown successively. The Si δ-doped layer with a concentration of 1×10^{18} cm^{-3} inside the upper barrier has a width of 6 nm and is 4 nm above the well. The sample was patterned to a 400 μm × 200 μm Hall bar by photolithography and wet etching. Indium was thermally burned onto the electrode pads to form Ohmic contacts. Magneto-transport experiments were done utilizing ac lock-in technique with 1 μA current and 13.333 Hz frequency under Oxiford Helium-4 superconducting system with a base temperature of 1.4 K. The sample stage is able to rotate so as to form a tilt angle between the normal of the sample surface and the direction of the magnetic field.

2 Results and discussion

The SdH oscillation of the longitudinal resistance R_{xx}, together with the transverse resistance R_{xy} showing quantum Hall plateaus, is shown in Fig. 1. Fitting with low field data gives the electron concentration $n_{\mathrm{Hall}} = 1.14 \times 10^{12}$ cm^{-2} and mobility $\mu = 3.07 \times 10^4$ cm^2/(V·s), which are typical for 2DESs lying in InGaAs QWs. The zero resistance of R_{xx} in high magnetic field indicates a negligible parallel conductance. It is weird that small dips emerge near the turning points where R_{xy} leaves the plateaus for the slope and that a small disturbance corresponding to the one at the highest plateau also appears. This phenomenon doesn't always occur for every measurement and is probably caused by the disfunction of the ac lockin amplifiers, e.g., due to phase jitters. Whether there exist any subtle mechanisms to account for this, it is beyond our concern here.

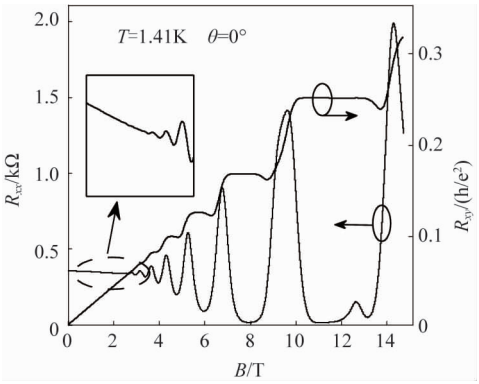

Fig. 1 SdH oscillations and the QHE of the sample. The measurements were taken in perpendicular magnetic field ($\theta = 0°$) at temperature = 1.41 K
图 1 样品的 SdH 振荡和量子霍尔效应。在垂直磁场($\theta = 0°$)和温度 $T = 1.41$ K 的条件下测量得到

A distinct feature of our sample can be seen from the behavior of R_{xx}: the absence of SdH beating effect, which is amazingly unexpected since previous magneto-transport experiments of similar InGaAs/InAlAs QWs have always reported the existence of SdH beating effect whenever the zero-field spin splitting is finite[5,8,11].

The absence of beating obliterates the possibility of extracting zero-field spin splitting via analyzing the beating nodes. Then we have to turn to the WAL effect. SOIs, which raise zero-field spin splittings, lead to spin relaxations that destroy the coherent backscattering of electrons moving along time-reversal-symmetrical paths, resulting in an excessive reduction of the weak localization (WL)[12], i.e., WAL. WAL usually manifests itself as the quantum correction to the classical Drude conductivity, $\Delta\sigma(B) = \sigma(B) - \sigma_0/(1 + \mu^2 B^2)$, where B is the magnetic field, μ is the electron mobility and σ_0 is the zero-field conductivity. We measured and ploted the conductivity correction of our sample in Fig. 2. Assuming that Rashba SOI dominates[13], we fitted the curve with Golub's model[14], which is quite suitable for high mobility samples[13,15]:

$$\Delta\sigma = \sigma_a(B, \tau_{tr}/\tau_\varphi, \Omega\tau_{tr}) + \sigma_b(B, \tau_{tr}/\tau_\varphi, \Omega\tau_{tr}), \quad (1)$$

where σ_a and σ_b represent contributions from backscattering and non-backscattering, respectively, τ_{tr} and τ_φ

are the transport scattering time and electron dephasing time, respectively, and Ω is the angular frequency of the Larmore precession caused by the SOI induced effective magnetic field. The two parameters involved in the fitting procedure are τ_φ and Ω, while τ_{tr} can be extracted from the mobility $\mu_{tr} = e\tau_{tr}/m^*$ with an effective mass $m^* = 0.051m_0$ (m_0 is the electron rest mass)[16]. Since the zero-field spin splitting Δ_0 is related to Ω by $\Delta_0 = 2\hbar\Omega$ ($\hbar$ is the reduced Planck constant), we obtained the Rashba splitting of our sample, $\Delta_0 = 1.97$ meV, which is comparable with that of similar InGaAs/InAlAs QWs[5, 8].

As is demonstrated here, a finite zero-field spin splitting doesn't guarantee the appearance of SdH beatings, implying a more subtle mechanism for its explanation. However, this is not the first time for the failure of observing SdH beatings. Although it is natural for symmetical QWs that no beatings should be observed due to lack of SIA (thus vanishing zero-field spin splitting)[17-18], absence of SdH beatings does occur when zero-field spin splitting is not zero[19-21]. Koga *et al.*[19] pointed out their failure of observing SdH beatings in their InGaAs/InAlAs QW samples and attributed it to the invisibility of SdH oscillations below $B = 2$ T, caused by the huge difference between the single-particle relaxation time τ_s and the transport scattering time τ_{tr}, since the last beating node would occur below $B = 1.5$ T. Gilbertson *et al.*[20] reported the absence of SdH beatings in their InSb/InAlSb asymmetric QWs and demonstrated that it was the large LL broadening that served as the cause. They also analysed the influence of spin-dependent scattering on SdH beatings and found that it leads to spin-dependent LL broadening and results in non-zero beating node amplitude, which may also hinder the observation of SdH beatings. Both of the above explanations may account for our case. Spirito *et al.*[21] investigated the transport properties of AlGaN/GaN heterostructures and showed that beatings dissappeared for an ungated sample but did appear for another gated sample, the reason for which was not determined in their paper. We also tested a gated sample cut from the same wafer, but we were still unable to observe the SdH beatings. Besides, Averkiev *et al.*[22] discussed theorectically the effects of the competing between Dresselhaus and Rashba SOIs on the beatings. They showed that beatings occur with either of the two SOIs dominating, but are strongly suppressed when the strength of them are close to each other. It is obvious that their theory doesn't suit our case since Rashba SOI dominates in our sample. It is also worth noting that beatings were not observed in some InAs/AlSb QWs but could be introduced by creating inhomogeneous carrier distributions via illuminating the samples[23]. However, the effect of inhomogeneities doesn't guarantee the rising of beatings[24] and has less to do with our case.

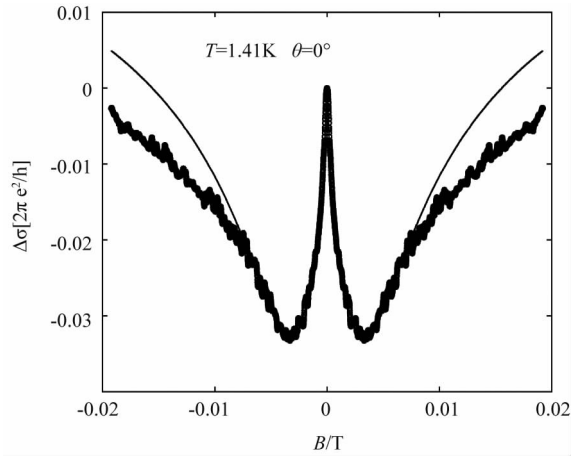

Fig. 2 Quantum correction to magnetoconductivity of the sample at $T = 1.41$ K and $\theta = 0°$. The solid curve is a fitting to the experimetal data using Golub's model

图2 样品在 $T = 1.41$ K 和 $\theta = 0°$ 的条件下的磁电导的量子修正。其中实线是用 Golub 模型拟合的结果

In order to disdinguish the possible mechnism for the absence of SdH beatings, we check the Dingle plot[25] that is shown in Fig. 3. Since the amplitude of SdH oscillations is given by[25]

$$\Delta R_{xx} = 4R_0 \exp\left(-\frac{\pi}{\omega_c\tau_q}\right)\frac{\chi}{\sin\chi} \quad , \quad (2)$$

where ΔR_{xx} is the SdH amplitude, R_0 is the zero-field resistance, ω_c is the cyclotron angular frequency, τ_q is the quantum scattering time, and $\chi = 2\pi^2 k_B T/\hbar\omega_c$ with k_B being the Boltzman constant and T the temperature, the Dingle plot is expected to be linear. Howerver, it is obvious that the "curve" deviates from a linear line type as the magnetic field B increases. Similar high-field bending in the Dingle plot has already been observed and attributed to either an inhomogeneous carrier distribution or a Gaussian line shape of the LLs[21,26]. We believe the former contributes less than the latter because our sample is of high quality. For a Gaussian line shape, the exponent part of the right hand in Eq. 2 should be replaced by $\exp\left[-\frac{\pi}{\mu_q^2}\left(\frac{1}{B}\right)\right]$, where $\mu_q = e\tau_q/m^*$ is the quantum mobility[26]. This results in a quadratic dependence on B^{-1} and is well verified by a parabolic fitting of the high field data as shown in Fig. 3. In Raikh and Shahbazyan's theorectical work[27], the LL broadening is confirmed to be Gaussian for high LL index when long-range scattering potential dominates. Considering our detailed sample structure, the long-range scattering potential can mainly come from the doping Be atoms whose effects are originally unintended. This may give a clue to the absence of SdH beatings.

It is interesting to look at the low field region of the Dingle plot. Although less convincing due to lack of enough data points, a slope change appears at about $B = 2.6$ T, indicating more than one conducting channel. This is in consistence with the previously confirmed finite zero-field spin splitting: the two conducting channels come from the two spin-splitted subbands. Spirito *et al.*[21] has used the slope change position to extract the zero-field spin splitting. Following their way and using $m^* = 0.051\ m_0$, we obtained a zero-field spin splitting of 2.95 meV, which is not far from the previous value obtained by WAL.

Next, we turn to the high field spin splitting of our sample. Fig. 4 shows the evolution of R_{xx} in tilted mag-

netic fields. As can be seen, the last two R_{xx} peaks at the filling factor $\nu = 5$ and $\nu = 7$ tend to split as the tilt angle θ increases, indicating a growing Zeeman splitting with θ. It must be pointed out that no obvious alternations between R_{xx} peaks and valleys are observed except at $\nu = 5$, due to limitations of our experimental conditions. Even at $\nu = 5$, the emerging valley doesn't complete itself, since it is expected to reach the "ground" where R_{xx} vanishes. Therefore, the widely used coincidence method[28] of extracting the effect g-factor, g^* (or the spin susceptibility $m^* g^*$) can not be applied to our sample.

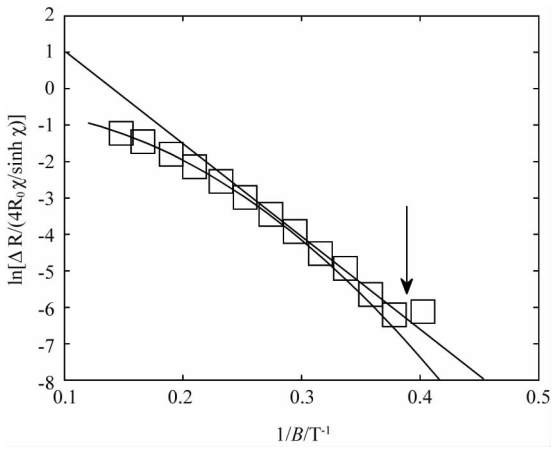

Fig. 3 Dingle plot of the sample. The solid line is a guide for the eyes and the solid curve is a parabolic fitting to the high field data. The arrow indicates the slope change position

图 3 样品的 Dingle plot 图。其中实直线是为人眼指示线,实曲线是对高场数据的拟合结果。箭头指示斜率突变的位置

In spite of the above restriction, we can still extract g^* in high magnetic field. The splitting of R_{xx} peak at $\nu = 5$ signals that the Fermi level E_F consecutively passes by the spin-resolved LL, thus, by noting that the peak splitting starts at $\nu = 7$ and becoming prominent only at $\nu = 5$, which means that the total spin splitting is much less than the energy interval between adjacent LLs, there is[29]

$$E_F = (N + \frac{1}{5})\hbar\omega_{c1} + \frac{1}{2}|g^*|\mu_B B_1) = (N + \frac{1}{2})\hbar\omega_{c2} - \frac{1}{2}|g^*|\mu_B B_2 \quad , \quad (3)$$

where N is the LL index, $\omega_{c1} = eB_i\cos\theta/m^*$ $(i = 1, 2)$ is the cyclotron angular frequency, μ_B is the Bohr magneton, $B_i (i = 1, 2)$ is the total magnetic field at which the splitted R_{xx} peaks appear. The above equation can be rewritten for our purpose ($N = 2$ for $\nu = 5$) as

$$\frac{B_{\perp 2} - B_{\perp 1}}{B_{\perp 2} + B_{\perp 1}} = \frac{|m^* g^*|\mu_B}{5\hbar e}\frac{1}{\cos\theta} \quad , \quad (4)$$

where $B_{\perp i} = B_i\cos\theta (i = 1, 2)$ is the perpendicular component of the total magnetic field B_i. Instead of extracting $|m^* g^*|$ at a single tilt angle, and by assuming that $|m^* g^*|$ has no dependence on θ, we linearly fitted the above equation, as shown in Fig. 5, and obtained $|m^* g^*| = (0.471 \pm 0.001) m_0$.

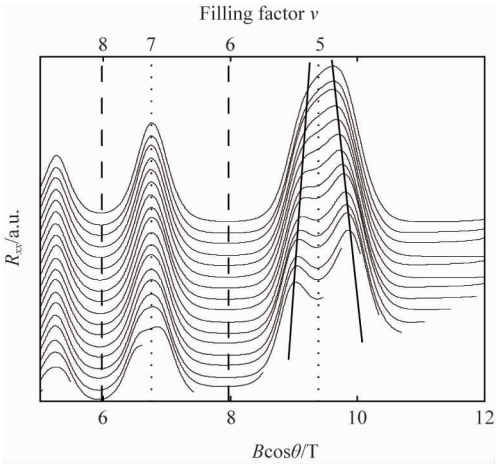

Fig. 4 Longitudinal magnetoresistance R_{xx} in tilted magnetic fields versus the perpendicular component of the total magnetic field $B_\perp = B\cos\theta$ at $T = 1.41$ K. All the curves are vertically shifted for clarity. The tilt angles for curves from uppermost to the bottom are 0°, 3.7°, 7.5°, 17.0°, 23.5°, 28.3°, 32.2°, 35.4°, 38.0°, 40.5°, 42.6°, 44.5°, 46.2°, 47.8°, 49.2°, 54.0°, 59.0°, 62.7°, 67.6°, 69.5°. The vertical dash (dotted) lines indicate the position of even (odd) filling factors. The two solid lines near $\nu = 5$ are guides for the eyes and indicate the evolution of peak positions with increasing tilt angle θ

图 4 样品在 $T = 1.41$ K 和倾斜磁场中的径向磁阻 R_{xx} 对磁场垂直分量 $B_\perp = B\cos\theta$ 的作图。所有的曲线均被竖直上移以便清晰显示。从上往下的倾斜角度为 0°, 3.7°, 7.5°, 17.0°, 23.5°, 28.3°, 32.2°, 35.4°, 38.0°, 40.5°, 42.6°, 44.5°, 46.2°, 47.8°, 49.2°, 54.0°, 59.0°, 62.7°, 67.6°, 69.5°。其中竖直的短横间隔线(点间隔线)指示偶数(奇数)填充因子。在 $\nu = 5$ 附近的两条斜直线指波峰的位置随倾斜角度 θ 的变化

The fitting is nearly perfect, which corroborates our assumption. This differs completely from Savel'ev *et al.*'s[29] results for a 2DES at the InGaAs/InP interface, which indicate a θ-dependent g^*. While they attributed it to the effects of the broadening and overlapping of spin-split LLs caused by disorder in their non-ideal 2DES, it seems that our sample doesn't suffer from this problem.

By dividing with the previously used effective mass, $m^* = 0.051 m_0$, the value of $|g^*|$ is calculated to be 9.24 ± 0.02. However, the effective mass used here may not be the accurate one for our sample, since it differs in a variety of samples due to variations in detailed band profiles, sample structures and electron concentrations. While the bulk $In_{0.53}Ga_{0.47}As$ has an effective mass of $0.043 m_0$ extracted by cyclotron resonace[30], the one for 2DESs in $In_{0.53}Ga_{0.47}As/In_{0.52}Al_{0.48}As$ QWs or heterojuctions is usually larger due to quantum confinement and nonparabolicity. Nitta *et al.*[8] reported an energy-dependent m^* ranging from $0.049 m_0$ to $0.052 m_0$ for a 20 nm QW for an electron concentration from 1.6×10^{12} cm^2 to 2.4×10^{12} cm^2. However, to our knowledge,

the lowest and highest m^* are reported to be $0.041m_0$[19] and $0.057\ 6m_0$[31], respectively. Thus, for m^* ranging from $0.041m_0$ and $0.0576m_0$, $|g^*|$ ranges from 8.18 to 11.49. This value of $|g^*|$ is much larger than the bulk $In_{0.53}Ga_{0.47}As$ $g^*=3$, as well as the low-field value of $|g^*|$ ranging from 2.62[16] to 3.8[32] extracted by other methods. However, it is well in the range of high-field $|g^*|$ extracted by coincidence method in the report of Nicholas et al[33]. As in their report, such high-field $|g^*|$ is well enhanced by exchange interaction and depends on the total spin polarization[29,33-34]:

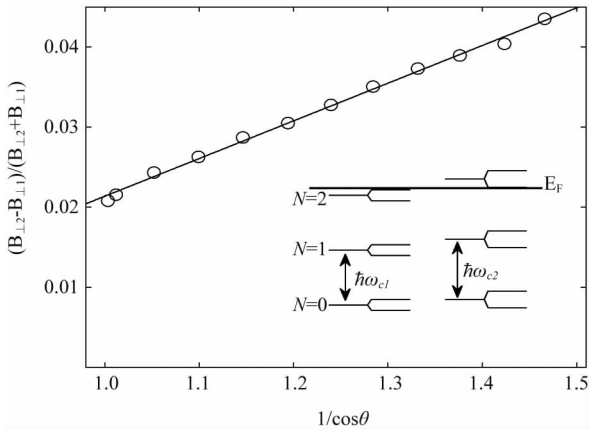

Fig. 5 Plot of $\frac{B_{\perp 2}-B_{\perp 1}}{B_{\perp 2}+B_{\perp 1}}$ against $1/\cos\theta$. The data points are extracted from the positions of spin-splitted R_{xx} peaks around $\nu=5$ (see Fig. 4). The inset illustrates the Fermi level E_F consecutively passing by the spin-splitted LLs

图5 $\frac{B_{\perp 2}-B_{\perp 1}}{B_{\perp 2}+B_{\perp 1}}$对 $1/\cos\theta$ 的作图。其数据点是在 $\nu=5$ 附近从自旋分裂的 R_{xx} 峰的位置得到的(见图4)。其中内插图演示费米能级 E_F 连续地越过自旋分裂的朗道能级

$$|g^*|\mu B = |g_0|\mu_B B + E_{ex}^0|n_\uparrow - n_\downarrow| \quad , \quad (5)$$

where g_0 is the bare g-factor excluding the effect of exchange interaction, E_{ex}^0 is the exchange constant and $n_\uparrow - n_\downarrow$ is the difference between the electon concentrations of the spin-up and spin-down subbands. If we adopt $|g_0| = 2.9$[29] and $|g^*| = 8.18 \sim 11.49$, and $|n_\uparrow - n_\downarrow| = D$ ($D = eB_\perp/2\pi\hbar$ is the spin-splitted LL degeneracy) for $\nu=5$ and $\theta=0°$, there is $E_{ex}^0 = (12.6 \sim 20.6) \times 10^{12}$ meV · cm^2, which is a little larger than that of AlGaAs/GaAs heterojunctions[34].

3 Conclusion

In summary, we investigated the magnetotransport properties of an asymmetrical $In_{0.53}Ga_{0.47}As/In_{0.52}Al_{0.48}As$ quantum well. The longitudinal magnetoresistance R_{xx} shows no beating pattern while zero-field spin splitting is confirmed to be non-zero by WAL. By fitting the θ-dependence of the spacing of spin-splitted R_{xx} peaks, we obtained the high-field effetive g-factor, $|g^*| = 8.18 \sim 11.49$, which is strongly enhanced by exchange interaction and has no dependence on θ. A nonlinear Dingle plot is analysed to further evidence the finite zero-field spin splitting and to emphasize the effect of long-range scattering potential from the doping Be atoms near the subtrate.

Acknowledgements

This work was supported in part by the Special Funds for Major State Basic Research under Project Nos. 2012CB619203 and 2013CB922301, the National Natural Science Foundation of China under Grant Nos. 11174306 and 61290304, the Innovation Program of Shanghai Institute of Technical Physics of the Chinese Academy of Sciences under Grant No. Q-ZY-76.

References

[1] Zutic I, Fabian J, Das Sarma S. Spintronics: Fundamentals and applications[J]. *Rev. Mod. Phys.* 2004, **76**(2):323.
[2] Ando T, Fowler A B, Stern F. Electronic properties of two-dimensional systems[J]. *Rev. Mod. Phys.* 1982, **54**(2):437.
[3] Radantsev V F. Spin effects in the magneto-oscillations of the capacitance of a two-dimensional gas of semiconductors with Kane and Dirac spectra[J]. *J. Exp. Theor. Phys.* 1999, **88**(3):552 - 560.
[4] Minkov G M, Germanenko A V, Larionova V A, *et al*. Tunneling studies of two-dimensional states in semiconductors with inverted band structure: Spin-orbit splitting and resonant broadening[J]. *Phys. Rev. B* 1996, **54**(3):1841.
[5] Das B, Miller D C, Datta S, *et al*. Evidence for spin splitting in $In_xGa_{1-x}As/In_{0.52}Al_{0.48}As$ heterostructures as $B\to0$[J]. *Phys. Rev. B* 1989, **39**(2):1411.
[6] Datta S, Das B. Electronic analog of the electro-optic modulator[J]. *Appl. Phys. Lett.* 1990, **56**(7):665.
[7] Bychkov Y A, Rashba E I. Oscillatory effects and the magnetic susceptibility of carriers in inversion layers[J]. *J. Phys. C Solid State Phys.* 1984, **17**(33):6039.
[8] Nitta J, Akazaki T, Takayanagi H, *et al*. Gate control of spin-orbit interaction in an inverted $In_{0.53}Ga_{0.47}As/In_{0.52}Al_{0.48}As$ heterostructure [J]. *Phys. Rev. Lett.* 1997, **78**(7):1335 - 1338.
[9] Studenikin S A, Coleridge P T, Yu G, *et al*. Electron spin-orbit splitting in a InGaAs/InP quantum well studied by means of the weak-antilocalization and spin-zero effects in tilted magnetic fields[J]. *Semicond. Sci. Technol.* 2005, **20**(11):1103 - 1110.
[10] De Andrada E Silva E A, La Rocca G C, Bassani F. Spin-split subbands and magneto-oscillations in III-V asymmetric heterostructures[J]. *Phys. Rev. B* 1994, **50**(12):8523.
[11] Hu C. -M, Nitta J, Akazaki T, *et al*. Zero-field spin splitting in an inverted $In_{0.53}Ga_{0.47}As/In_{0.52}Al_{0.48}As$ heterostructure: Band nonparabolicity influence and the subband dependence[J]. *Phys. Rev. B* 1999, **60**(11):7736 - 7739.
[12] Germanenko A V. Spin effects and quantum corrections to the conductivity of two-dimensional systems[J]. *Low Temp. Phys.* 2009, **35**(1):24.
[13] Faniel S, Matsuura T, Mineshige S, *et al*. Determination of spin-orbit coefficients in semiconductor quantum wells[J]. *Phys. Rev. B* 2011, **83**(11):115309.
[14] Golub L. Weak antilocalization in high-mobility two-dimensional systems[J]. *Phys. Rev. B* 2005, **71**(23):235310.
[15] Yu G, Dai N, Chu J, *et al*. Experimental study of the spin-orbit quantum interference effect in a high-mobility $In_xGa_{1-x}As/InP$ quantum well structure with strong spin-orbit interaction[J]. *Phys. Rev. B* 2008, **78**(3):035304.
[16] Liu X Z, Xu Y G, Yu G, *et al*. The effective g-factor in $In_{0.53}Ga_{0.47}$

$As/In_{0.52}Al_{0.48}As$ quantum well investigated by magnetotransport measurement[J]. *J. Appl. Phys.* 2013, **113**(3):033704.

[17] Schapers Th, Engels G, Lange J, *et al*. Effect of the heterointerface on the spin splitting in modulation doped $In_xGa_{1-x}As/InP$ quantum wells for $B\to 0$[J]. *J. Appl. Phys.* 1998, **83**(8):4324.

[18] Cui L J, Zeng Y P, Wang B Q, *et al*. Zero-field spin splitting in $In_{0.52}Al_{0.48}As/In_xGa_{1-x}As$ metamorphic high-electron-mobility-transistor structures on GaAs substrates using Shubnikov-de Haas measurements [J]. *Appl. Phys. Lett.* 2002, **80**(17):3132.

[19] Koga T, Nitta J, Akazaki T, *et al*. Rashba spin-orbit coupling probed by the weak antilocalization analysis in InAlAs/InGaAs/InAlAs quantum wells as a function of quantum well asymmetry[J]. *Phys. Rev. Lett.* 2002, **89**(4):046801.

[20] Gilbertson A M, Branford W R, Fearn M, *et al*. Zero-field spin splitting and spin-dependent broadening in high-mobility $InSb/In_{1-x}Al_xSb$ asymmetric quantum well heterostructures[J]. *Phys. Rev. B* 2009, **79**(23):235333.

[21] Spirito D, Frucci G, Di Gaspare D, *et al*. Quantum transport in low-dimensional AlGaN/GaN systems[J]. *J. Nanoparticle Res.* 2010, **13**(11):5699-5704.

[22] Averkiev N S, Glazov M M, Tarasenko S A. Suppression of spin beats in magneto-oscillation phenomena in two-dimensional electron gas[J]. *Solid State Commun.* 2005, **133**(8):543-547.

[23] Brosig S, Ensslin K, Warburton R J, *et al*. Zero-field spin splitting in InAs-AlSb quantum wells revisited[J]. *Phys. Rev. B* 1999, **60**(20): R13989.

[24] Syed S, Manfra M J, Wang Y J, *et al*. Electron scattering in AlGaN/GaN structures electron scattering in AlGaN/GaN structures[J]. *Appl. Phys. Lett.* 2004, **84**(9):1507.

[25] Coleridge P T. Small-angle scattering in two-dimensional electron gases[J]. *Phys. Rev. B* 1991, **44**(8):3793.

[26] Spirito D, Di Gaspare L, Frucci G, *et al*. Magnetotransport investigation of conducting channels and spin splitting in high-density AlGaN/AlN/GaN two-dimensional electron gas[J]. *Phys. Rev. B* 2011, **83**(15):155318.

[27] Raikh M E, Shahbazyan T V. High Landau levels in a smooth random potential for two-dimensional electrons[J]. *Phys. Rev. B* 1993, **47**(3):1522-1531.

[28] Fang F F, Stiles P J. Effects of a tilted magnetic field on a two-dimensional electron gas[J]. *Phys. Rev.* 1968, **174**(3):823.

[29] Savelév I G, Kreshchuk A M, Novikov S V, *et al*. Spin splitting of the Landau levels and exchange interaction of a non-ideal two-dimensional electron gas in $In_xGa_{1-x}As/InP$ heterostructures[J]. *J. Phys.: Condens. Matter* 1996, **8**(46):9025-9036.

[30] Portal J C, Nicholas R J, Brummell M A, *et al*. Quantum transport in GaInAs-AlInAs heterojunctions, and the influence of intersubband scattering[J]. *Solid State Commun.* 1982, **43**(12):907.

[31] Lo I, Cheng J P, Chen Y F, *et al*. Effective mass of two-dimensional electron gas in δ-doped $Al_{0.48}In_{0.52}As/Ga_{0.47}In_{0.53}As$ quantum wells [J]. *J. Appl. Phys.* 1996, **80**(6):3355.

[32] Nitta J, Lin Y, Akazaki T, *et al*. Gate-controlled electron g factor in an InAs-inserted-channel $In_{0.53}Ga_{0.47}As/In_{0.52}Al_{0.48}As$ heterostructure [J]. *Appl. Phys. Lett.* 2003, **83**(22):4565.

[33] Nicholas R J, Brummell M A, Portal J C, *et al*. An experimental determination of enhanced electron g-factors in GaInAs-AlInAs heterojunctions[J]. *Solid State Commun.* 1983, **45**(10):911-914.

[34] Englert T H, Tsui D C, Gossard A C, *et al*. g-Factor enhancement in the 2D electron gas in GaAs/AlGaAs heterojunctions[J]. *Surf. Sci.* 1982, **113**(1-3):295-300.